# *A Comparison of Corner and Saliency Detection Methods for Power Line Detection*

*Ömer Emre YETGİN*
*Department of Electrical and Electronics Engineering*
*Anadolu University*
*Eskişehir, TURKEY*
*omeremreyetkin@gmail.com*

*Ömer Nezih GEREK*
*Department of Electrical and Electronics Engineering*
*Anadolu University*
*Eskişehir, TURKEY*
*ongerek@anadolu.edu.tr*

***Abstract*— Issuing an alarm for power lines continues to be an important issue for low altitude aircraft safety. In this study, edge and gradient based methods are applied and compared according to their detection performances (in terms of Accuracy, F-Score, Speed and False Negative). It was observed that; despite being used genuinely for corners, HARRIS method provides significantly superior accuracy and F-Score for infrared images, and SIFT method provides superior accuracy and F-Score for visible light images. Interestingly, FAST method provides superior speed and false negative rate for both infrared and visible light images.**

***Index-Terms-Power line detection, line detection, obstacle detection, aircraft safety, corner detection.***

## I. INTRODUCTION

Cables and power lines impose a big safety threat for low altitude aircrafts. Most of the avoidance work is left to the pilot, making the system prone to human errors. Camera and vision based systems are relatively new issues to aid the pilot regarding automated powerline detection. For both humans and vision systems, low contrast and confusion between cables and the background remains to be problems. The current method to warn helicopter pilots is to use colored spheres that are attached to the power cables (as seen in Fig.1) [1, 2]; however, these warning labels are not densely used everywhere. The desired automated system is expected to have high detection accuracy with as low false positives as possible, and is expected to be computationally fast. Normally, civil helicopters travel at an average speed of 135 knots (meaning that it covers 200 meters in 3 seconds). This necessitates the automatic system to react at a distance of at least 200 meters [2].

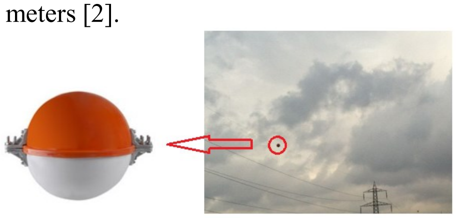

Fig.1. Warning sphere for power lines [2].

The recent vision based alarm generation methods use saliency approaches, where cable locations are emphasized to aid pilots [3,4,5]. Despite being oldest saliency indicators, edge and corner detection methods have not been thoroughly analyzed and compared before. This work presents comparison of a wide class of edge, corner and saliency detection methods over a large set of actual aerial scenes with and without power lines. We briefly describe the used methods and present experimental results.

## II. AERIAL IMAGE DATABASE

There are several works that aim to detect power lines or warn the pilot [6-12]. Quite unfortunately, these works use mostly artificially generated images, with almost no infrared (IR) imaging examples. The authors cooperated with the Turkish Electricity Transmission Company (TEIAS) to videos from real aircrafts (as shown in Fig.2) and extract a valuable image corpus (Fig.3).


Fig.2. Airborne imaging system projected by TEIAS. (a) External appearance of the helicopter (b) Imaging system [13,14].

In this work, 20 visible light (VL) and 20 IR images (10 from each group containing power lines) are selected from this Power Line Database [15,16] and scaled to a size of 512x512.

## III. CORNER AND SALIENCY DETECTION METHODS

Several valuable saliency detection methods are incorporated in corner detection algorithms. Hence, we preferred to incorporate popular corner detection methods in the set of comparison herein.

978-1-5386-1880-6/17/$31.00 ©2017 IEEE

*A. FAST*

FAST Corner Detector is a popular method that detects significant salient points [17].

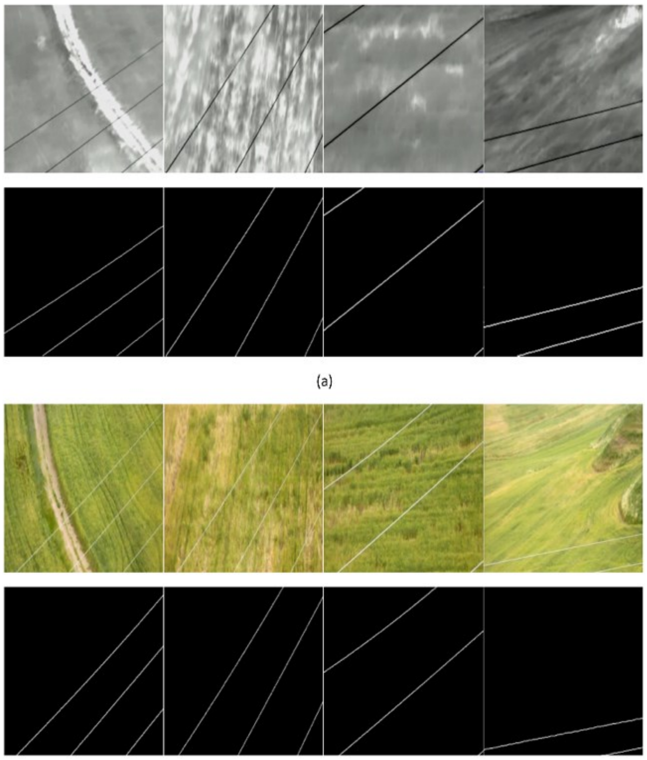

Fig.3. (a) IR and Ground Truth images (b) VL and Ground Truth images [16].

The method checks a candidate pixel, *p,* according to a threshold, *T,* using the following algorithm:

1. Select 16 pixels around *p* in a radius of 3 pixels [18].
2. Compare these 16 pixels to *p*. If a consecutive set of *N* pixels is altogether different from *p* by an amount *T*, mark *p* as a corner.

In order to improve the speed, a multiresolution variant is used. First, pixels indexed as 1, 5, 9, and 13 are selected among these 16 pixels and if at least 3 of them do not satisfy the threshold condition, candidate *p* is eliminated. Else, the algorithm continues checking for the remaining 12 pixels. A final non maximal suppression method is applied to eliminate multiple neighboring corner detection. Fig.4 shows examples of FAST corner detection results.

*B. HARRIS*

Harris is perhaps the most popular corner/saliency detection method [19]. It is a gradient-based method that comes out to be fast and scale/rotation invariant. It starts by calculating a local gradient estimate:

$$E(u,v) = \sum_{x,y} w(x,y)\,[I(x+u,y+v) - I(x,y)]^2 \quad [19]$$

where, $I(x,y)$ is the intensity image, $w(x,y)$ is the local window, and $(u,v)$ is the shift vector. Places with large $E$ values are candidates for corners. By defining the M matrix with gradient estimate as:

$$M = \sum_{x,y} w(x,y) \begin{bmatrix} {I_x}^2 & I_x I_y \\ I_x I_y & {I_y}^2 \end{bmatrix} \quad [19]$$

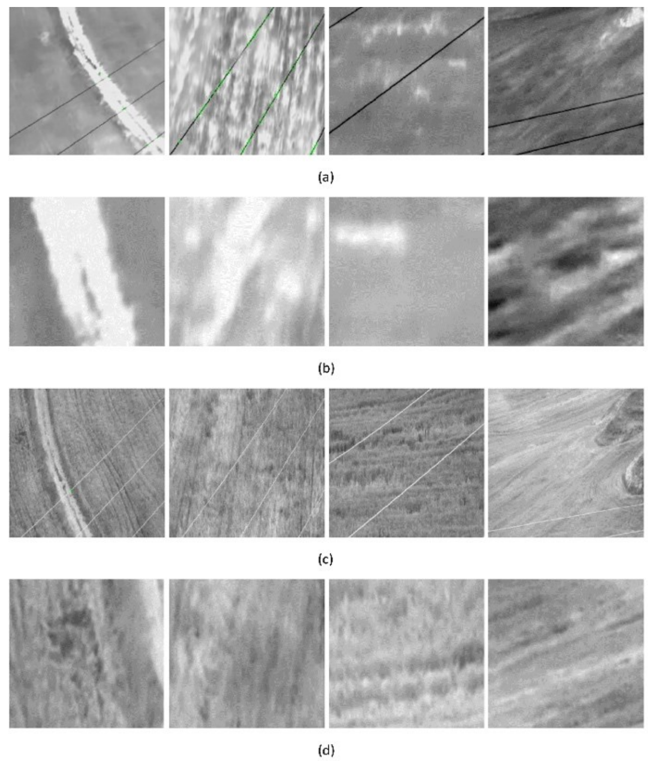

Fig.4. (a) IR (Powerline inside) and (b) IR (No powerline inside) results of FAST algorithms, (c) VL (Powerline inside) and (d) VL (No powerline inside) results of FAST algorithms.

which makes a gradient estimate as:

$$E(u,v) \approx [u \quad v]\, M \begin{bmatrix} u \\ v \end{bmatrix} \quad [19]$$

The quantity that is compared against a threshold becomes:

$$R = \det M - k\,(trace\ M)^2 \quad [19]$$

Sample results for Harris Corner Detection are shown in Fig.5.

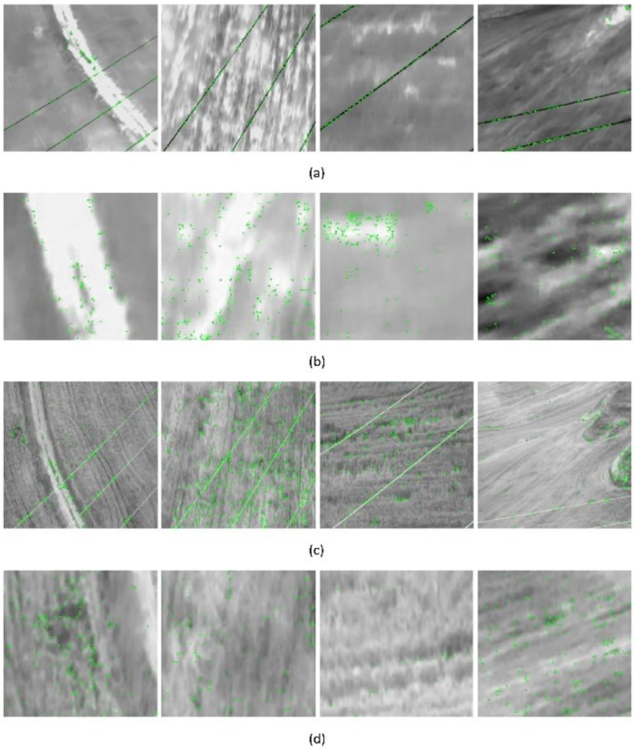

Fig.5. (a) IR (Powerline inside) and (b) IR (No powerline inside) results of HARRIS algorithms, (c) VL (Powerline inside) and (d) VL (No powerline inside) results of HARRIS algorithms.

## C. The Shi-Tomasi Corner Detector (MinEigenValue)

Shi-Tomasi Corner Detector is a Harris-like method that basically replaces the comparison quantity [20]. In Harris, the $R$ quantity is evaluated with $det\, M = \lambda_1 \lambda_2$ and $trace\, M = \lambda_1 + \lambda_2$, whereas in Shi-Tomasi, the quantity is simply determined as $R = min(\lambda_1, \lambda_2)$. Fig.6 shows sample results for Shi-Tomasi corner detection labels.

## D. SIFT (Scale Invariant Feature Transform)

SIFT is a versatile tool that produces features that are invariant to scaling, rotation and illumination [21]. This popular method first detects scale-spaces extrema by difference of Gaussian (DoG) method that is applied to the image at various scales. Then, the number of salient points is reduced by accurate keypoint localization [8].

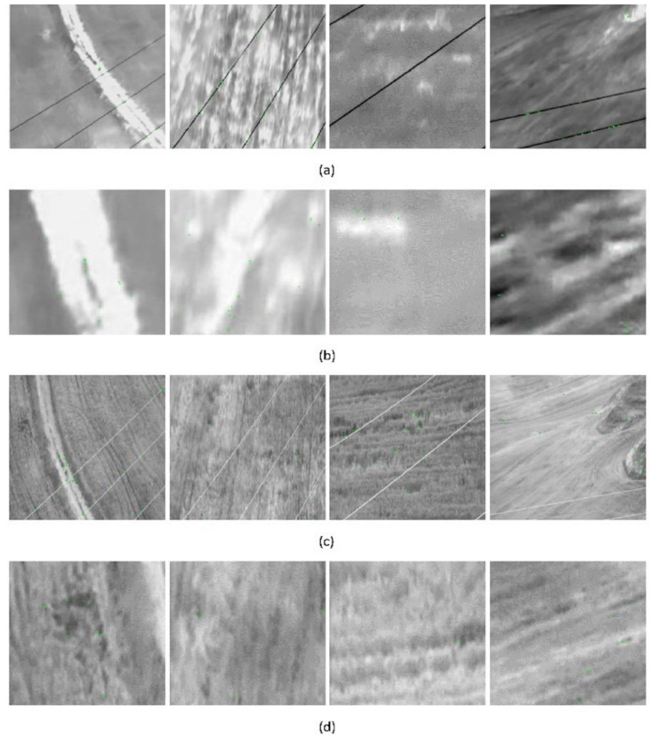

Fig.6. (a) IR (Powerline inside) and (b) IR (No powerline inside) results of Shi-Tomasi algorithms, (c) VL (Powerline inside) and (d) VL (No powerline inside) results of Shi-Tomasi algorithms.

DoG function naturally attains high values along edge positions and small values along its perpendicular. We generate the following Hessian matrix that estimates directional first differences:

$$H = \begin{bmatrix} D_{xx} & D_{xy} \\ D_{xy} & D_{yy} \end{bmatrix} \quad [21]$$

SIFT, then considers the maximum eigenvalue (α) to minimum eigenvalue (β) ratio (*r*) using a simple fact that:

$$\frac{Tr(H)^2}{Det(H)} = \frac{(\alpha+\beta)^2}{\alpha\beta} = \frac{(r\beta+\beta)^2}{r\beta^2} = \frac{(r+1)^2}{r} \quad [21]$$

takes a minimum when the two eigenvalues are the same and increases as the eigenvalue ratio increases.

The final stage is to determine the local gradient direction for each keypoint. Using the Gaussian smoothed image $L(x, y)$, the gradient magnitude $m(x, y)$ and gradient direction $\theta(x, y)$ can be evaluated as:

$$m(x,y) = \sqrt{(L(x+1,y) - L(x-1,y))^2 + \left(L(x,y+1) - L(x,y-1)\right)^2}$$

$$\theta(x,y) = tan^{-1}\left(\frac{L(x,y+1)-L(x,y-1)}{L(x+1,y)-L(x-1,y)}\right) \quad [21]$$

The orientations are quantized to 8 main directions for each 4x4 cell points around the keypoint. Then, a 128-bin histogram is evaluated as the feature vector. In order to eliminate illumination effects, the histogram is normalized. Fig.7 shows examples of SIFT method outcomes.

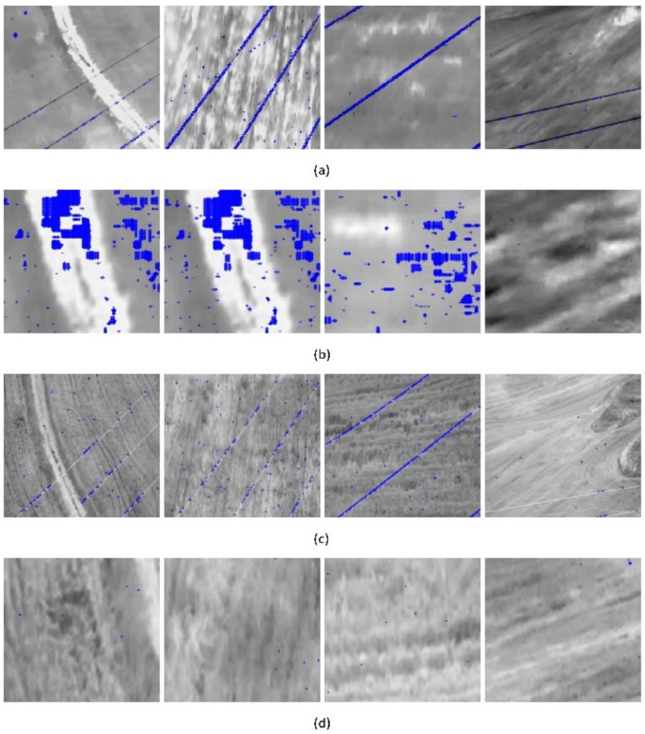

Fig.7. (a) IR (Powerline inside) and (b) IR (No powerline inside) results of SIFT algorithms, (c) VL (Powerline inside) and (d) VL (No powerline inside) results of SIFT algorithms.

### *E. SURF (Speeded Up Robust Features)*

SURF method focuses its attention to saliency structures in the image [22]. Such structures can normally be found around corners of objects or speckles of light. The following steps summarize the algorithm:

1. Find image interest points (using Hessian matrix)
2. Find major interest points in scale space (using non-maximal suppression on scaled interest point maps)
3. Find feature "directions"
4. Generate feature vectors

Unlike SIFT, SURF uses integral images, therefore runs faster. Besides, it uses Haar transform for robustness agains luminance variations. Fig.8 shows example results of SURF.

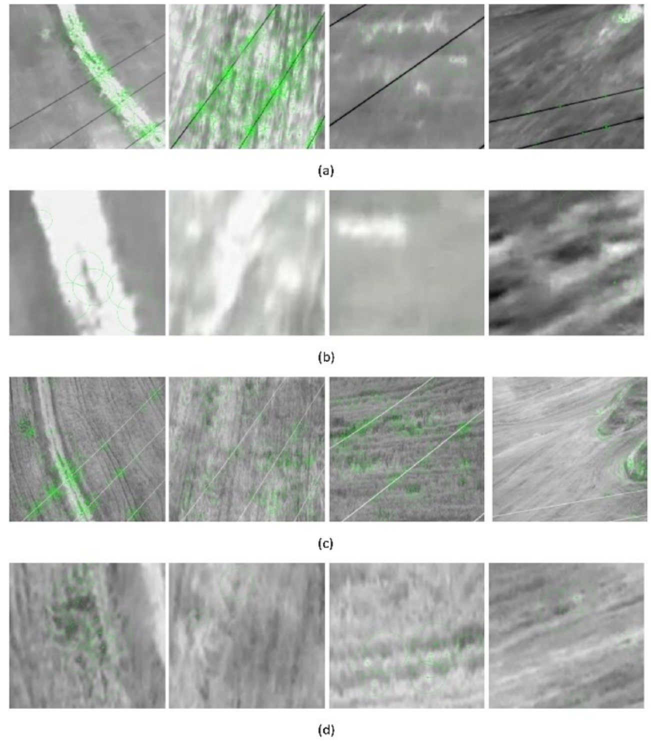

Fig.8. (a) IR (Powerline inside) and (b) IR (No powerline inside) results of SURF algorithms, (c) VL (Powerline inside) and (d) VL (No powerline inside) results of SURF algorithms.

## IV. RESULTS AND CONCLUSIONS

Using the above described methods, we performed experiments on actual IR and VL images. The results are compared according to accuracy, F-Score, speed and FN; and presented in Tables 1 – 4. General inspection of Tables 1 and 2 show that the maximum accuracy and F-Score were achieved using IR images with "Harris Corner Detector" (Accuracy of 96.50%, F-Score of 0.99). On the VL side, the maximum accuracy and F-Score were achieved using VL image database with "SIFT" (Accuracy of 77.95%, F-Score of 0.86).

Tables 3 shows that the fastest of these method is the FAST method (around 0.1 sec.) using MATLAB interpreter on a regular (2.8 GHz i7 processor and 16 GB RAM) laptops. Considering the speed requirements of the application (1 – 3 sec.), these methods are observed to be very satisfactory, even on MATLAB. Tables 4 shows that False Negative (FN) for IR and VL image database with FAST method is an ideal 0 %. We conclude that Corner and Saliency Detection Methods provide a plausible alternative for power line detection.

TABLE 1. COMPARISON OF ACCURACY TABLE OF IR AND VL IMAGES (%-MEAN) (POWERLINE INSIDE)

| METHODS | IR | VL |
|---|---|---|
| FAST | 68,57 | 10 |
| HARRIS | **96,50** | 55,97 |
| Shi-Tomasi | 87,57 | 48,71 |
| SIFT | 87,55 | **77,95** |
| SURF | 66,36 | 53,56 |

TABLE 2. COMPARISON OF F-SCORE TABLE OF IR AND VL IMAGES (MEAN) (POWERLINE INSIDE)

| METHODS | IR | VL |
|---|---|---|
| FAST | 0,69 | 0,1 |
| HARRIS | **0,99** | 0,68 |
| Shi-Tomasi | 0,89 | 0,61 |
| SIFT | 0,92 | **0,86** |
| SURF | 0,73 | 0,66 |

TABLE 3. COMPARISON OF SPEED (SECONDS-MEAN) TABLE OF IR AND VL IMAGES (SECONDS-MEAN) (POWERLINE INSIDE)

| METHODS | IR | VL |
|---|---|---|
| FAST | **0,11** | **0,10** |
| HARRIS | 0,16 | 0,17 |
| Shi-Tomasi | 0,18 | 0,15 |
| SIFT | 2,50 | 2,48 |
| SURF | 0,12 | 0,12 |

TABLE 4. COMPARISON OF FN RATE (%-MEAN) TABLE OF IR AND VL IMAGES (NO POWERLINE INSIDE)

| METHODS | IR | VL |
|---|---|---|
| FAST | **0** | **0** |
| HARRIS | 60 | 0,1296 |
| Shi-Tomasi | 2,78 | 0,0030 |
| SIFT | 1,24 | 0,0038 |
| SURF | 0,0005 | 0,0064 |

## ACKNOWLEDGMENT

This work is supported by Anadolu University Scientific Research Project Commission under the grant No. 1508F598. The authors would like to thank Turkish Electricity Transmission Company for providing power line videos. The authors also thank Assistant Professor Cihan TOPAL for his valuable support in technical issues.

## REFERENCES

[1] Yetgin, O.E and Gerek, O,N., “Cable and Wire Detection System for Aircrafts”, Signal Processing and Communications Applications Conference (SIU), 2013.

[2] Yetgin, O.E., Şentürk, Z. and Gerek, O.N., "A Comparison of Line Detection Methods for Power Line Avoidance in Aircrafts", 9th International Conference on Electrical and Electronics Engineering (ELECO), 2015.

[3] Gandhi, T., Yang M. T., Kasturi, R., Camps, O., Coraor, L. and McCandless, J., “Detection of obstacles in the flight path of an aircraft”, IEEE Trans. Aerospace and Electronic Systems, vol. 39, no. 1, pp. 176–191, 2003.

[4] Avizonis, P., Barron, B., “Low cost wire detection system”, Digital Avionics Systems Conference, vol. 1, 1999, 3.C.3-1-3.

[5] Kurdila, A., Nechyba, M., Prazenica, R., Dahmen, W., Binev, P., DeVore, R., Sharpley, R., “Vision-based control of micro-air-vehicles”, Conf. Decision and Control, 2004.

[6] Yonemoto, N., et al., "Performance of obstacle detection and collision warning system for civil helicopters." Defense and Security Symposium. International Society for Optics and Photonics, 2006.

[7] Yan, G., et al., "Automatic extraction of power lines from aerial images." IEEE Geoscience and Remote Sensing Letters 4.3, 2007 : 387-391.

[8] Candamo, J., et al., "Detection of thin lines using low-quality video from low-altitude aircraft in urban settings." IEEE Transactions on Aerospace and Electronic Systems 45.3, 2009 : 937-949.

[9] Li, Z., et al., "Towards automatic power line detection for a UAV surveillance system using pulse coupled neural filter and an improved Hough transform." Machine Vision and Applications 21.5, 2010 : 677.

[10] Ma, Q., et al., "An algorithm for power line detection and warning based on a millimeter-wave radar video." IEEE Transactions on Image Processing 20.12, 2011 : 3534-3543.

[11] Liu, Y., Mejias, L. and Li, Z., "Fast power line detection and localization using steerable filter for active UAV guidance.", In 12th International Society for Photogrammetry & Remote Sensing (ISPRS2012), 2012.

[12] Martinez, C., et al., "Towards autonomous detection and tracking of electric towers for aerial power line inspection." Unmanned Aircraft Systems (ICUAS), 2014 International Conference on. IEEE, 2014.

[13] TEIAS imaging helicopter appearing in: http://www.kaanair.com/tr/haberler_detay.aspx?ID=151, 2016.

[14] TEIAS imaging helicopter appearing in: http://www.teias.gov.tr/ebulten/haberler/2013/eih%20helikopter/HELIKOPTER.html, 2016.

[15] Yetgin, Ömer Emre; GEREK, Ömer Nezih, “Power Line Image Dataset (Infrared-IR and Visible Light-VL)”, Mendeley Data, v7, http://dx.doi.org/10.17632/n6wrv4ry6v.1, 2017.

[16] Yetgin, Ömer Emre; Gerek, Ömer Nezih, “Ground Truth of Powerline Dataset (Infrared-IR and Visible Light-VL)”, Mendeley Data, v8, http://dx.doi.org/10.17632/twxp8xccsw.8, 2017.

[17] Rosten, Edward, and Tom Drummond. "Fusing points and lines for high performance tracking." Tenth IEEE International Conference on Computer Vision (ICCV'05) Volume 1. Vol. 2. IEEE, 2005.

[18] D. Hearn, M. Pauline Baker, Computer Graphics, 2nd Edition, Prentice-Hall, Englewood Cli!s, NJ, 1997, pp. 97-102.

[19] Harris, Chris, and Mike Stephens. "A combined corner and edge detector." Alvey vision conference. Vol. 15. 1988.

[20] Shi, Jianbo, and Carlo Tomasi. "Good features to track." Computer Vision and Pattern Recognition, 1994. Proceedings CVPR'94., 1994 IEEE Computer Society Conference on. IEEE, 1994.

[21] Lowe, David G. "Object recognition from local scale-invariant features." Computer vision, 1999. The proceedings of the seventh IEEE international conference on. Vol. 2. Ieee, 1999.

[22] Bay, Herbert, Tinne Tuytelaars, and Luc Van Gool. "Surf: Speeded up robust features." European conference on computer vision. Springer Berlin Heidelberg, 2006.